para-Azaquinodimethane: a Versatile Quinoidal Moiety for Functional Materials Discovery

Xuncheng Liu,[#,‡] Christopher L. Anderson,[†,$,‡] Yi Liu[†,&*]

[†]The Molecular Foundry and [&]Materials Sciences Division, Lawrence Berkeley National Laboratory, One Cyclotron Road, Berkeley, California, 94720, USA

[#]College of Materials and Metallurgy, Guizhou University, Guiyang 550025, P. R. China

[$]Department of Chemistry, University of California, Berkeley, Berkeley, CA, 94720, USA

Conspectus:

The past 50 years of discovery in organic electronics have been driven in large part by the donor-acceptor design principle, wherein electron-rich and electron-poor units are assembled in conjugation with each other to produce small band gap materials. While the utility of this design strategy is undoubtable, it has been largely exhausted as a frontier of new avenues to produce and tune novel functional materials to meet the needs of the ever-increasing world of organic electronics applications. Its sister strategy of joining quinoidal and aromatic groups in conjugation has—by comparison—received much less attention, in large part due to the categorically poor stability of quinoidal conjugated motifs.

In 2017 though, the *para*-azaquinodimethane (AQM) motif was first unveiled, which showed a remarkable level of stability despite being a close structural analog to *para*-quinodimethane—a notably reactive compound. In contrast, dialkoxy AQM small molecules and polymers are stable even under harsh conditions and could thus be incorporated into conjugated polymers. When polymerized with aromatic subunits, these AQM-based polymers show notably reduced band gaps that follow reversed structure-property trends to some of their donor-acceptor polymer counterparts and yield organic field-effect transistor (OFET) hole mobilities above 5 cm^2

V^{-1} s^{-1}. Additionally, in an ongoing study, these AQM-based compounds are also showing promise as singlet fission (SF) active materials due to their mild diradicaloid character.

An expanded world of AQMs was accessed through their ditriflate derivatives, which were first used to produce ionic AQMs (iAQMs) sporting two directly attached cationic groups that significantly affect the AQM motif's electronics—producing strongly electron-withdrawing quinoidal building blocks. Conjugated polyelectrolytes (CPEs) created with these iAQM building blocks exhibit optical band gaps stretching into the near infrared I (NIR-I) region and showed exemplary behavior as photothermal therapy agents.

In contrast to these stable AQM examples, the synthetic exploration of AQMs also produced examples of more typical diradicaloid reactivity—but in forms that were controllable and produced intriguing and high-value products. With certain substitution patterns, AQMs were found to dimerize to form highly-substituted [2.2]paracyclophanes in distinctly more appreciable yields than typical cyclophane formation reactions. Certain AQM ditriflates, when crystallized, undergo light-induced topochemical polymerization to form ultra-high molecular weight (>10^6 Da) polymers that showed excellent performances as dielectric energy storage materials. These same AQM ditriflates could be used to produce the strongly electron-donating redox-active pentacyclic structure: pyrazino[2,3-*b*:5,6-*b'*]diindolizine (PDIz). The PDIz motif allowed for the synthesis of exceedingly small band gap (0.7 eV) polymers with absorbances reaching all the way into the NIR-II region that were also found to produce strong photothermal effects.

Both as stable quinoidal building blocks and through their controllable diradicaloid reactivity, AQMs have already proven to be versatile and effective as functional organic electronics materials.

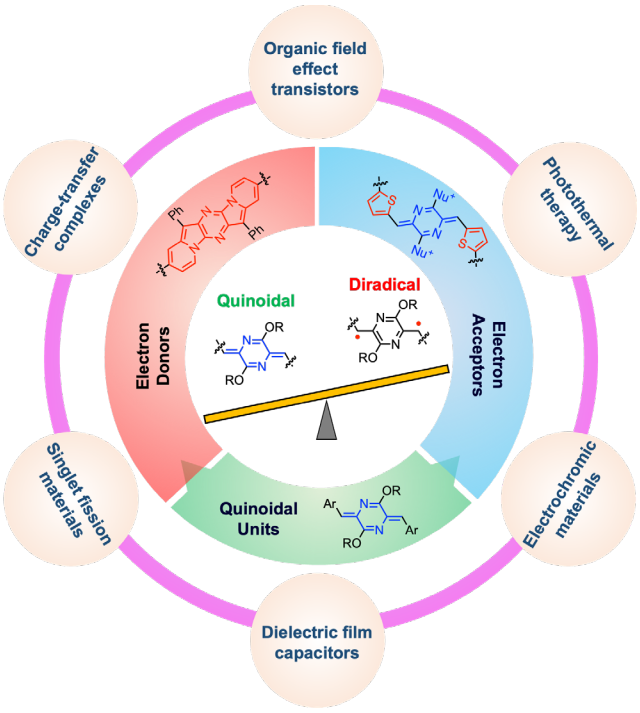

Key references:

- Liu, X.; He, B.; Anderson, C.; Kang, J.; Chen, T.; Chen, J.; Feng, S.; Zhang, L.; Kolaczkowski, M.; Teat, S.; Brady, M.; Zhu, C.; Wang, L.; Chen, J.; Liu, Y. "*para*-Azaquinodimethane: a Compact Quinodimethane Variant as an Ambient Stable Building Block for High Performance Low Band Gap Polymers", *J. Am. Chem. Soc.* **2017**, *139*, 8355-8363.[1] This work reported the discovery of *para*-azaquinodimethane unit and its use in low band gap quinoidal-donor conjugated polymers.
- Anderson, C. L.; Dai, N.; Teat, S.; He, B.; Wang, S.; Liu, Y. "Electronic Tuning of Mixed Quinoidal-Aromatic Conjugated Polyelectrolytes via Direct Ionic Substitution", *Angew. Chem. Int. Ed.* **2019**, *58*, 17978-17985.[2] New chemistry enables the versatile functionalization of *para*-azaquinodimethanes for use as ionic electron acceptors.
- Anderson, C. L.; Li, H.; Jones, C. G.; Teat, S. J.; Settineri, N. S.; Dailing, E. A.; Liang, J.; Mao, H.; Klivansky, L. M.; Li, X.; Reimer, J. A.; Nelson, H. M.**;** Liu, Y. "Solution-

Processable and Functionalizable Ultra-high Molecular Weight Polymers via Topochemical Synthesis", *Nat. Commun.* **2021**, *12*, 6818.[3] The diradical characters of *para*-azaquinodimethanes were activated for polymerization in molecular crystals to afford processible, ultra-high molecular weight polymers.

- Liang, H.; Liu, C.; Zhang, Z.; Liu, X.; Zhou, Q.; Zheng, G.; Gong, X.; Xie, L.; Yang C.; Zhang, L.; He, B.; Chen, J.; Liu, Y. "Unravelling the Role of Electron Acceptors for the Universal Enhancement of Charge Transport in Quinoid-Donor-Acceptor Polymers for High-Performance Transistors", *Adv. Funct. Mater.* **2022**, 2201903.[4] The *para*-azaquinodimethane unit has been adapted as an "electron-neutral" unit to implement a "quinoid-donor-acceptor" design, leading to conjugated polymers with tunable band gaps and high hole transport mobilities.

1. Introduction

Quinoidal compounds, represented by the archetypal *para*-quinodimethane (*p*-QM, Figure 1), are conjugated ring systems featuring exocyclic double bonds and alternating single and double bond patterns.[5-8] Despite the simple non-aromatic Lewis structure that is used to describe quinoidal compounds, the actual electronic states of these structures are much more complex due to the resonance between a closed-shell quinoidal form and an open-shell diradical benzenoidal form. The open-shell diradicaloid character is promoted by the strong driving force to recover aromaticity at the expense of the two exocyclic double bonds. Depending on the size and composition of the conjugated ring system, the ground state of quinoidal compounds may contain varying degrees of quinoidal and benzenoidal characters. This feature has stimulated numerous studies on the design and synthesis of quinoidal systems, which not only advance the fundamental

understanding of aromaticity, reactivity and ground-state multiplicity, but also engender intricate optical, electronic and magnetic properties suited for potential applications in organic electronics, non-linear optics, organic spintronics, and quantum information science.[6-7, 9-11] Quinoidal motifs are also well known for their ability to influence the electronic and optoelectronic properties in larger aromatic ring systems and small band gap conjugated polymers.[12-17]

Accompanying the electronic consequences of the quinoidal-aromatic resonance is an impact on the ambient stability of quinoidal compounds and therefore the practicality of their use in functional materials. This property is exemplified by *p*-QM **1** (Figure 1a), which behaves like a diradical and is notoriously reactive at ambient conditions—a property that is utilized to afford industrially useful parylene dielectric materials.[18] To stabilize the quinoidal character in a compound, two main strategies have been employed: end-capping the exocyclic groups with electron withdrawing groups,[19] and embedding the *p*-QM structural motif within an expanded polycyclic hydrocarbon π-system.[20] While these synthetic strategies have resulted in a plethora of exotic molecular systems with fine-tuned aromaticity and ground state multiplicity,[21-23] such chemical modifications are often synthetically demanding, complicating their use as synthons for materials. Even for the limited number of quinoid units that have been incorporated into conjugated polymers, they have been substituted with strongly electron-withdrawing stabilizing groups and have thus been primarily discussed in the context of electron acceptors while the quinoidal contribution to their electronic properties has been undervalued.[16, 24-27] As the applications of conjugated polymers grow, it has become more and more desirable to develop simple quinoidal units that are stable, electronically unbiased, structurally tunable and easy to synthesize, which will enable further use in novel conjugated systems.

In 2017, our group reported on a compact-sized quinoidal unit based on a *para*-azaquinodimethane (AQM) core (Figure 1b).[1] This motif contains two nitrogen atoms in its central six-membered ring system along with two *O*-alkylated substituents, and behaves as an ambient-stable quinoidal unit with little open-shell reactivity. The "electron-neutral" nature is evident from its high-lying lowest unoccupied molecular orbital (LUMO) energy level. When incorporated into conjugated polymers, the AQM motif imparts a unique quinoidal modulation of electronic structure and chain conformation in contrast to conventional donor-acceptor polymers. Consequently, semiconductors with high carrier mobility, small band gaps and singlet fission capability have been created using the AQM motif. Our subsequent studies on the chemical modification of AQMs have demonstrated that the AQM unit is a versatile quinoidal synthon for the design and synthesis of functional materials.

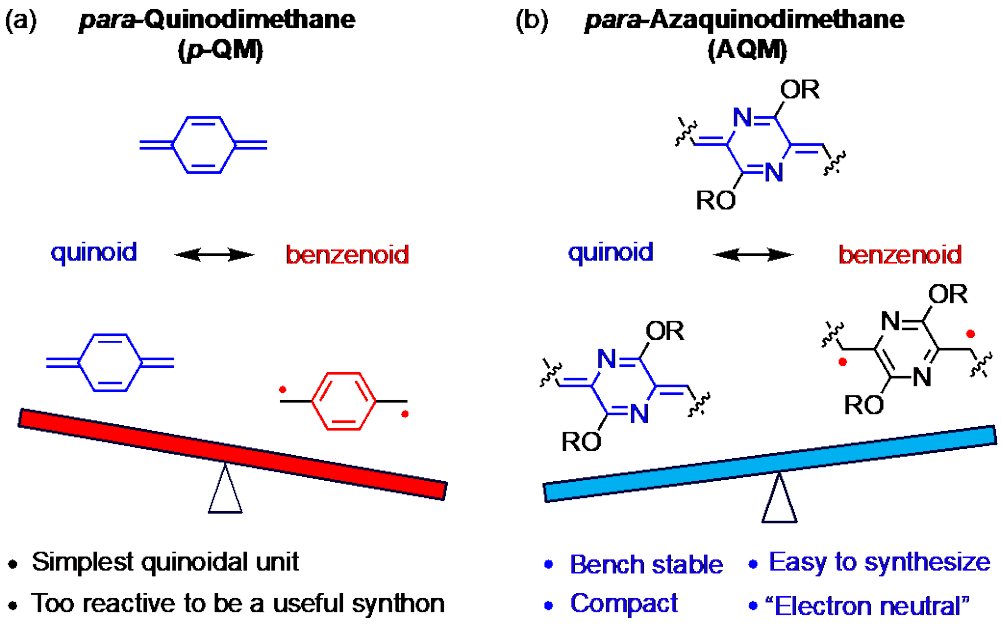

Figure 1. Structures of (a) *p*-QM and (b) AQM with their closed-shell quinoid and open-shell benzenoid electronic resonance forms.

2. Synthesis of the AQM core

The first formal synthesis of AQM derivatives was achieved in two simple and high yielding steps.[1] A representative synthesis is illustrated Scheme 1a, starting with the base-promoted Knoevenagel condensation reaction between *N*,*N*-diacetyl-2,5-diketopiperazine (AcDKP) and 2-formyl-5-bromothiophene (**1**), followed by alkylation with 1-hexylbromide under basic conditions. Notably, the arylidene **2** produced in this condensation reaction assumes exclusively a *Z*,*Z'*-configuration as a result of *N*-*O* acetyl transfer.[28] The subsequent alkylation step is crucial for the synthesis of the AQM core. In the presence of K_2CO_3, **2** is deprotonated to afford *N*-anions, which undergo spontaneous tautomerization to form *O*-anions and the quinoidal AQM ring. *O*-alkylation is the only process observed, affording AQM **3** in 61% yield with no *N*-alkylation product. This synthesis can be easily carried out on gram-scales and is quite modular, giving access to a range of AQMs bearing different aromatic and alkyl groups. AQMs bearing electron-donating aryl end groups such as thiophenes are bench stable under ambient conditions both in the solid state and in solution. The single crystal X-ray structure of **3** reveals that the AQM conjugated system is highly planar, with significant N•••S interactions that reinforce a planar conformation (Scheme 1b). Electrochemical measurements indicated that **3** has a LUMO energy of around -2.9 eV, considerably higher than that of medium strength electron acceptors such as benzothiadiazole.[29] This feature suggests that AQM is an "electron-neutral" quinoidal unit in contrast to most other quinoidal conjugated building blocks.

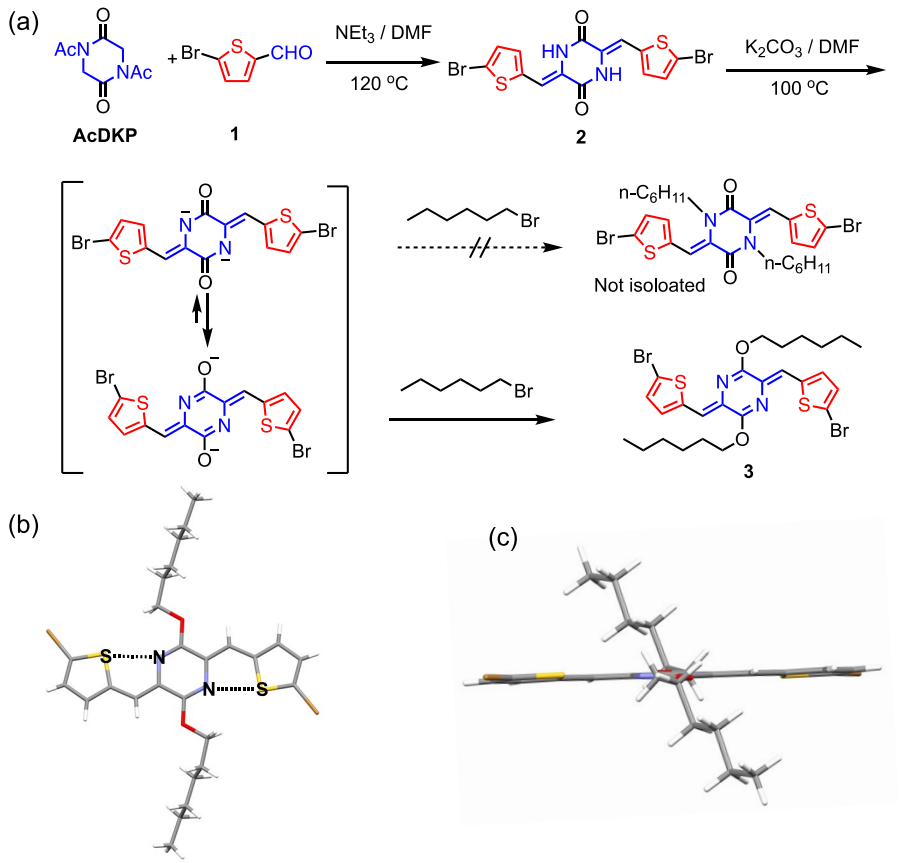

Scheme 1. (a) Synthesis of an AQM derivative **3** via the condensation-alkylation sequence. Single crystal X-ray structure of **3** showing (b) S•••N interactions and (c) the coplanar conformation. Adapted with permission from ref 1. Copyright 2017 American Chemical Society.

3. AQM-based Conjugated Polymers

3.1 The construction of quinoid-donor (Q-D) polymers

Mixed quinoid-donor conjugated polymers, such as those depicted in Scheme 2a, were anticipated to possess intriguing optical and electronic properties owing to the quinoidal resonance stabilization of their excited states. This is exemplified by the resonance between the quinoidal and aromatic forms of thiophene units, which is compensated for by the resonance between the AQM ring's quinoidal and aromatic pyrazine forms, leading to the reduction in bond-length

alternations along the polymer backbone and consequently a narrowed band gap. Design strategies that leverage such quinoidal-aromatic resonances are distinct from the commonly employed donor-acceptor approach, as manifested in a systematic study of a series of AQM-oligothiophene based Q-D conjugated polymers (Scheme 2b).[30] It is worth noting that AQM is an intrinsic quinoidal unit, which differs from pro-quinoidal building blocks such as thieno[3,4-b]thiophene (T*b*T), despite a similar quinoidal-aromatic resonating stabilizing effect when embedded within extended conjugated systems.[31]

The successful synthesis of the Q-D polymers exploited the excellent chemical stability of the alkoxy-substituted thiophene-flanked AQMs. AQM **4** displayed reactivity similar to conventional aromatic dibromide building blocks. AQM distannates could be obtained in high yields via *n*-BuLi-assisted halide exchange (Scheme 2b). From these, AQM-based polymers **P1**-**P3** with different lengths of oligothiophene spacers (n = 2, 3, or 4) and different solubilizing alkoxy sidechains could be obtained via Stille polycondensation.

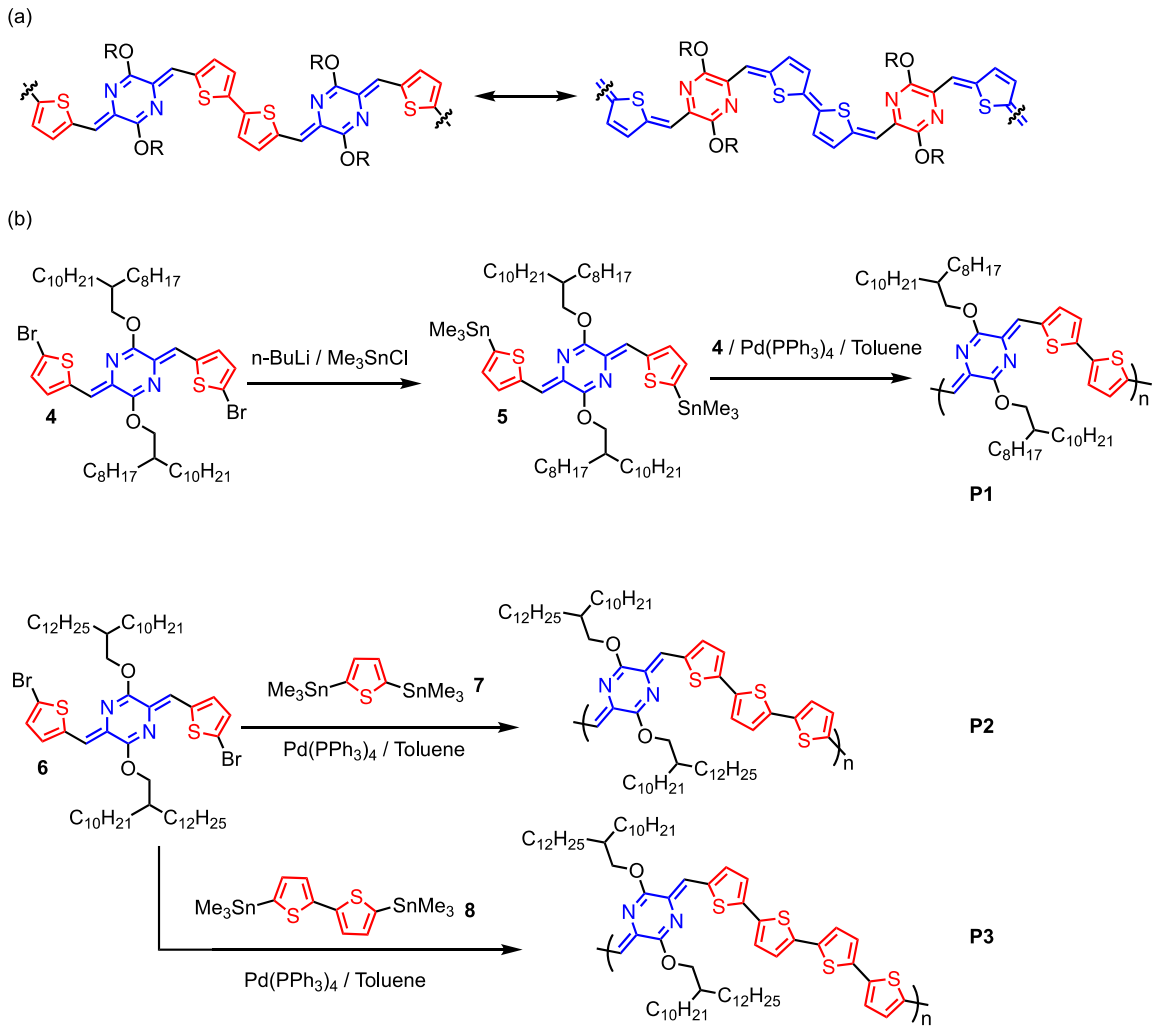

Scheme 2. (a) Minimization of bond length alternation via aromatic-quinoid resonance in AQM based Q-D polymers. (b) Synthesis of AQM-oligothiophene polymers **P1**-**P3** via Stille polycondensation. Adapted with permission from ref 1. Copyright 2017 American Chemical Society.

Comparison of the **P1**-**P3** series highlights the remarkable band gap tuning ability of the AQM unit. All polymers exhibit small band gaps, low LUMO energies, and high highest occupied molecular orbital (HOMO) energies (Figure 2a). Notably, **P1** has an optical band gap of 1.32 eV with an absorption edge at 938 nm, significantly smaller than that of conventional donor-acceptor

polymers based on naphthalene diimide (NDI), isoindigo (iID) and difluorobenzotriazole (FBTA) (Figure 2b). This feature suggests that the AQM motif is more effective at narrowing the HOMO-LUMO gap compared to those well-known electron acceptors despite its "electron-neutral" nature. Additionally, the band gaps of the quinoidal-aromatic alternating polymers follow the trend: **P1**<**P2**<**P3**, correlating with the increasing number of thiophenes in the repeating unit. This trend is the opposite of the trend observed in donor-acceptor polymers, where the band gaps decrease as the number of thiophenes increases due to the increase in their HOMO energy levels. These results are attributable to the dilution of the quinoidal resonance stabilization effect and suggest a reverse band gap engineering rule that differs from that used in the main-stream donor-acceptor approach.

AQM polymers were found to perform well as hole transporting materials in organic field effect transistors (OFETs). OFETs based on **P1–P3** with bottom-gate and top-contact exhibit hole mobilities up to 0.034, 0.54 and 0.084 $cm^2V^{-1}s^{-1}$, respectively. Comparable hole mobilities of AQM copolymers containing more rigid thieno[3,2-b]thiophene or thiophene vinylene thiophene units were reported by Schmaltz and coworkers.[32] Thanks to the conjugated geometry of the AQM polymer backbones and the low torsion angles between their AQM and oligothiophene units, the polymer chains are nearly fully planar, which facilitate both their packing into highly orientated lamellar domains and their inter-chain charge carrier transport in the solid state.

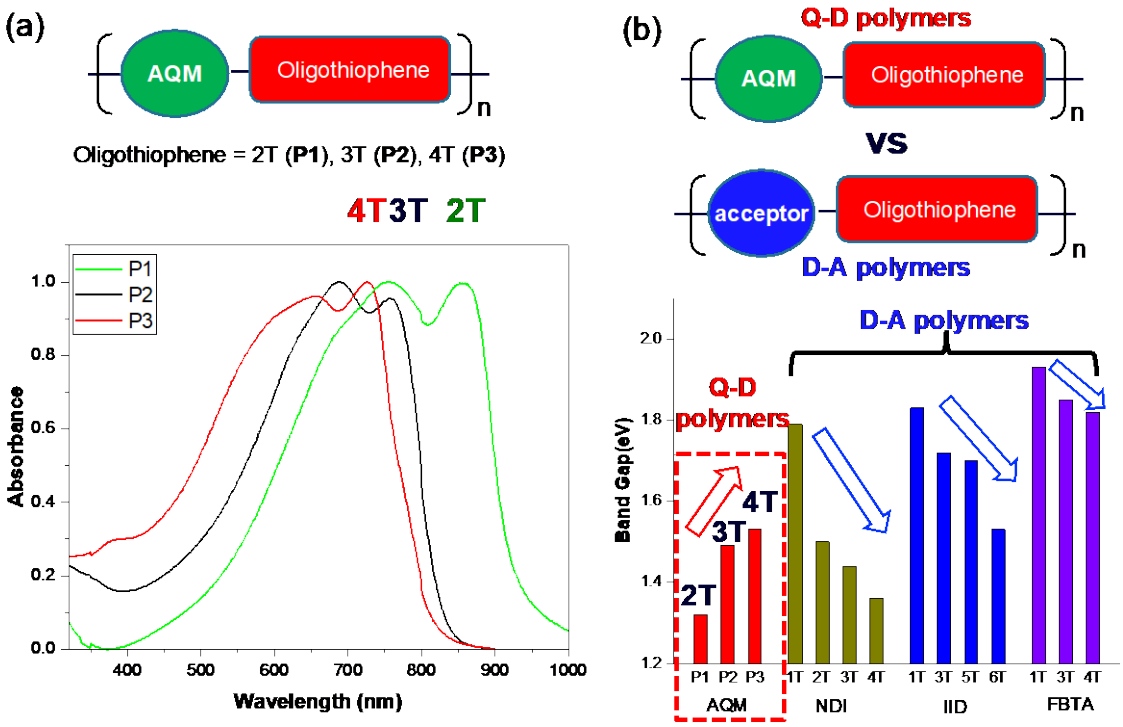

Figure 2. (a) Absorption spectra of **P1**-**P3**. (b) Comparison of AQM-based Q-D polymers and D-A polymers in terms of band gap and oligothiophene length. Adapted with permission from ref 1. Copyright 2017 American Chemical Society.

3.2 Structure-property relationships in Q-D polymers

Charge transport properties of conjugated polymers are strongly dependent on their chain packing behavior in thin films. Grazing incidence wide-angle x-ray scattering (GIWAXS) studies revealed that the orientations of the crystalline domains of **P1**-**P3** can vary drastically, with **P1** adopting a predominantly face-on orientation with the polymer lamella parallel to the substrate, while **P3** adopts a nearly pure edge-on orientation with the polymer lamella perpendicular to the substrate. Prompted by those initial results, further structure-morphology-property relationship studies were carried out on AQM-based Q-D polymers by systematically varying the main chain and sidechain structures.[33] Three series of small band gap Q-D polymers are shown in Figure 3 grouped based

on their polymer main chain structures, the branching point of their alkyl side chains, and the lengths of the branches of their alkyl chains. GIWAXS studies of the polymer thin film morphologies revealed high crystallinity in all samples. As the length of the oligothiophene subunit increases, the polymer crystallites transition from favoring a face-on to an edge-on orientation. A similar tendency was also observed when moving the branching point position away from the main chain of the AQM-terthiophene-based polymers, while the overall alkyl chain length had little impact on crystallite orientation. The orientation preference change is a consequence of the change in interchain interaction strength. Stronger interchain packing would weaken the polymer main chain-substrate interactions while the side chain-substrate interactions become dominant, leading to preferential edge-on orientation. The thin film morphologies of these AQM polymers correlate well with their corresponding charge transport behavior in OFET devices. The polymer with the branching point at the fourth carbon has the highest charge carrier mobility—exceeding 1.0 $cm^2V^{-1}s^{-1}$—which is concurrent with a bimodal packing pattern. This study provided a comprehensive description of the correlations between Q-D polymer structure, thin film morphology and device performance, highlighting the importance of regulation of molecular structure to achieve a desirable bimodal texture and highly ordered microstructures in thin films for better charge transport.

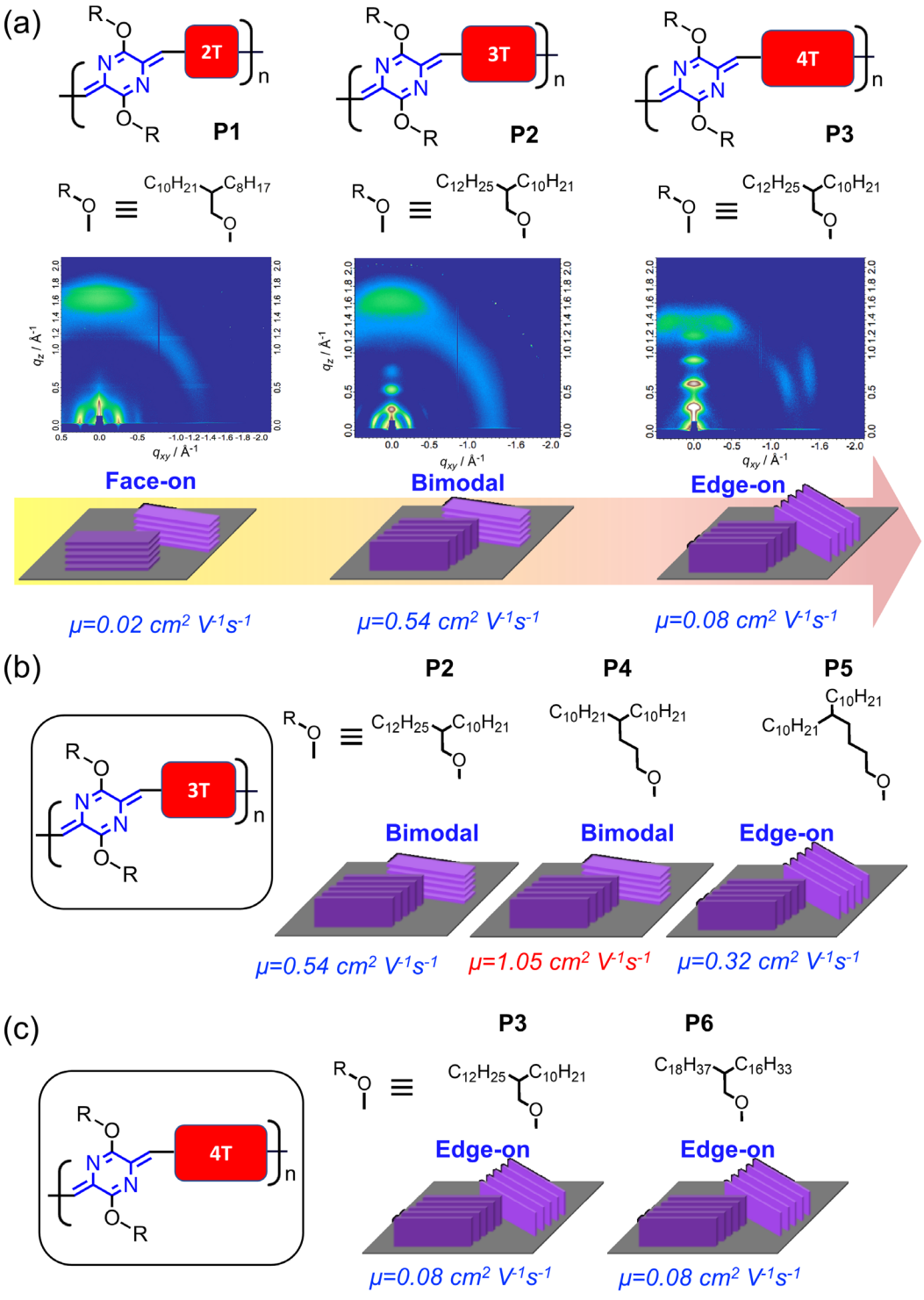

Figure 3. Comparison of thin film morphology and charge carrier mobilities of three series of AQM-based Q-D polymers. Adapted with permission from ref 33. Copyright 2018 John Wiley and Sons.

3.3 Q-D-A conjugated polymers: a general design strategy for band gap narrowing and carrier mobility enhancement

The resonance stabilization effect observed in AQM-based Q-D polymers inspired us to explore an alternative strategy to further tune the frontier orbital energy and intrinsic carrier transport properties (Figure 4a). By introducing an additional electron acceptor into the conjugated polymer backbone, a series of quinoid-donor-acceptor (Q-D-A) polymers were synthesized with a thiophene-AQM-thiophene-acceptor motif as the repeat unit (Figure 4b).[4, 34] The overall electronic properties of these polymers reflect the combined character of quinoidal-aromatic systems and donor-acceptor systems, resulting in narrower band gaps relative to the corresponding binary Q-D and D-A polymers. Compared to the Q-D polymer, the additional acceptor moiety in the repeat unit lowers the HOMO and LUMO energy levels simultaneously, as shown in Figure 4c, while also promoting more effective intra-chain charge transport and inter-chain charge hopping. Organic field-effect transistors based on these Q-D-A polymers exhibit excellent hole mobilities ranging from 0.71 to 5.10 $cm^2 V^{-1} s^{-1}$, which are orders of magnitude higher than the corresponding D-A and Q-D polymers (Figure 4d). Notably, the hole mobility of 5.10 $cm^2 V^{-1} s^{-1}$ of **P9** was among the highest for quinoidal-aromatic polymers. Furthermore, morphological studies by GIWAXS revealed that Q-D-A polymers with stronger acceptor units tend to form edge-on lamellas, exhibit high film crystallinity, small effective hole masses and excellent operational stability.[4]

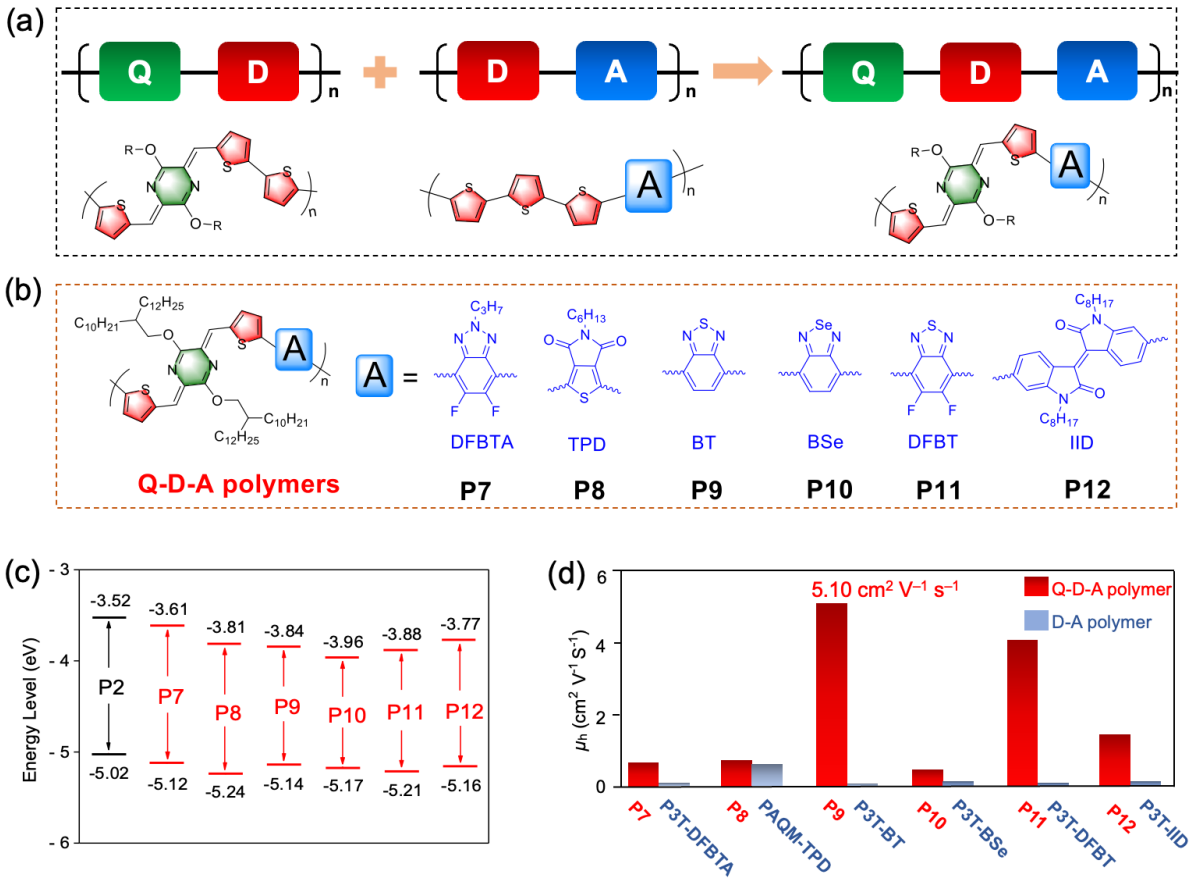

Figure 4. (a) Schematic diagram of the Q-D-A strategy. (b) A list of Q-D-A polymers **P7-P12** based on various acceptor units. (c) Diagram of the energy levels of Q-D polymer and Q-D-A polymers. (d) Comparison of maximum hole mobilities of Q-D-A polymers and the D-A counterparts. Adapted with permission from ref 4. Copyright 2022 John Wiley and Sons.

4. Modulating the electronic properties and reactivity of AQMs

As previously discussed, the formation of the AQM core hinges on its selective *O*-alkylation, which limits the 2,5-substituents to alkoxy groups only. To expand the scope of AQM chemistry, we developed a convenient one-step transformation that generates the quinoidal core while simultaneously introducing two triflate groups as functional handles for further chemical

transformations (Scheme 3). By treating thiophene- or phenylene-end capped cyclic bisamide **9** or **10** with triflic anhydride in the presence of pyridine, the corresponding AQM ditriflates **11** or **12** were obtained in nearly quantitative yields.[2-3] The successful transformation has set the stage for the exploration of versatile chemical transformations associated with the AQM ring system, thereby expanding the utility of AQM to broader applications.

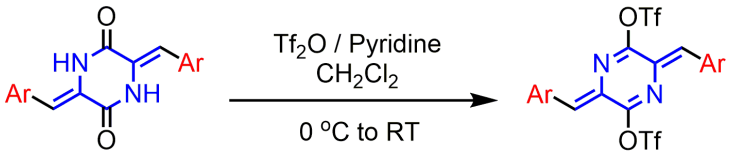

Starting material		Product		Yield
9 Ar =		**11** Ar =		98%
10 Ar =		**12** Ar =		95%

Scheme 3. Synthesis of AQM ditriflates with different end groups.

4.1 Strongly electron-withdrawing ionic AQMs and conjugated polyelectrolytes

One of the prominent outcomes of this AQM ditriflate chemistry is the formation of ionic AQMs (iAQMs) following their reaction with neutral nucleophiles such as substituted pyridines and triphenylphosphine (selected examples shown in Scheme 4).[2] In strong contrast to the alkoxy-derived AQMs which are electronically unbiased, iAQMs' electronic structures are strongly affected by the electron deficiency of their positively charged substituents, leading to significantly lowered LUMO energies and subsequently reduced band gaps and red-shifted absorption features compared to the neutral AQMs.[2] Triphenylphosphonium-appended iAQMs show lower LUMO energies and smaller band gaps compared to pyridinium-appended iAQMs and act as large, sterically-blocking groups, reducing their reactivity in various circumstances. When the π-

conjugation was extended along the axis of the AQM motif exocyclic methylenes by installing additional thiophene units, the optical band gap was further decreased due to modulation of frontier orbital energy levels via the conventional donor-acceptor principle. The ability to tune the electronic properties along both molecular axes of the AQM core provides an exquisite level of modularity that transforms the electronically neutral AQM into a strong ionic electron acceptor unit with low-lying LUMO levels often below -4.0 eV. Moreover, novel viologen conjugated iAQMs have been constructed following a similar protocol. They not only function as strong redox-active acceptor units but also show interesting host-guest interactions with hosts such as cucurbiturils (CBs), thanks to the unique viologen-quinoid construct.[35]

The strong electron-accepting properties of iAQMs have been harnessed to create ionic, ultra-narrow band gap conjugated polymers, such as **P13** and **P14**, that contain triphenylphosphonium appended iAQMs and terthiophene and quaterthiophene groups in their respective repeat units. These conjugated polyelectrolytes (CPEs) showcase the band gap reduction effects of combining the donor-acceptor strategy with the quinoid-modulated bond-length alternation reduction strategy. The optical band gaps of 1.22 and 1.33 eV for **P13** and **P14**, respectively, fall within the biologically relevant near infrared one (NIR-I) region. As a result, these conjugated polyelectrolytes exhibit excellent photothermal activities and high antibacterial efficacy as photothermal therapy agents.

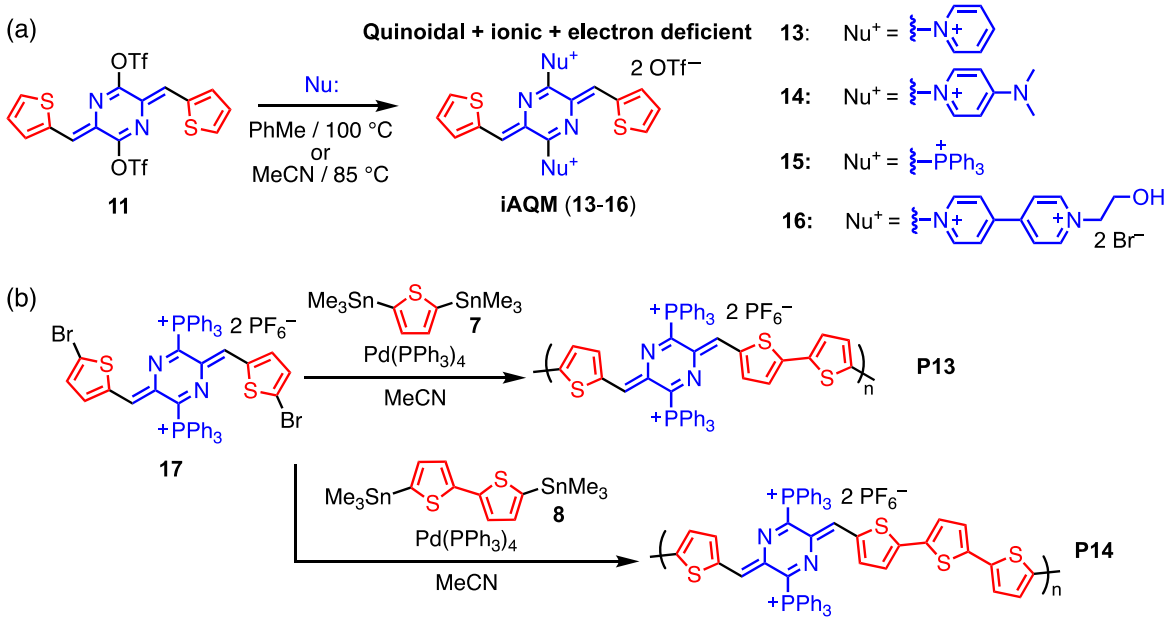

Scheme 4. (a) Synthesis of a variety of iAQMs via nucleophilic substitution. (b) Synthesis of iAQM-based small band gap conjugated polyelectrolytes.

4.2 Cross-coupling reactions of AQMs to form paracyclophanes

While all of the examples discussed so far indicate that the AQM ring is a highly stabilized quinodimethane derivative, certain substitution patterns also produce reactive AQMs. AQM triflates exhibit reactivity to common aryl stannates in metal-catalyzed cross-coupling reactions. For instance, the AQM triflate **11** reacted readily with 2-tributyltinthiophene under Stille coupling conditions (Scheme 5a).[36] The cross-coupling product **18**, however, could not be isolated due to its highly reactive biradical character. Instead, a highly substituted [2,2]paracyclophane **19** was obtained as a result of spontaneous dimerization of **18** in 25% yield. The calculated frontier molecular orbital density diagrams indicate significant electron density between the two pyrazine rings, suggesting a through-space conjugation effect.[37] The formation of **19** represents a valuable and highly substituted addition to the [2.2]paracyclophane family, which are notoriously challenging to synthesize in appreciable yields due to their high strain. Furthermore, the isolation

of **19** rather than the reactive intermediate **18** demonstrates the intricacies of stability in AQM derivatives. Importantly, this effect on the reactivity of the AQM ring cannot be explained simply by electronic factors, as the dialkoxy AQMs discussed previously are very stable—even at elevated temperatures—despite sharing a similar highly electron-donating substitution pattern.

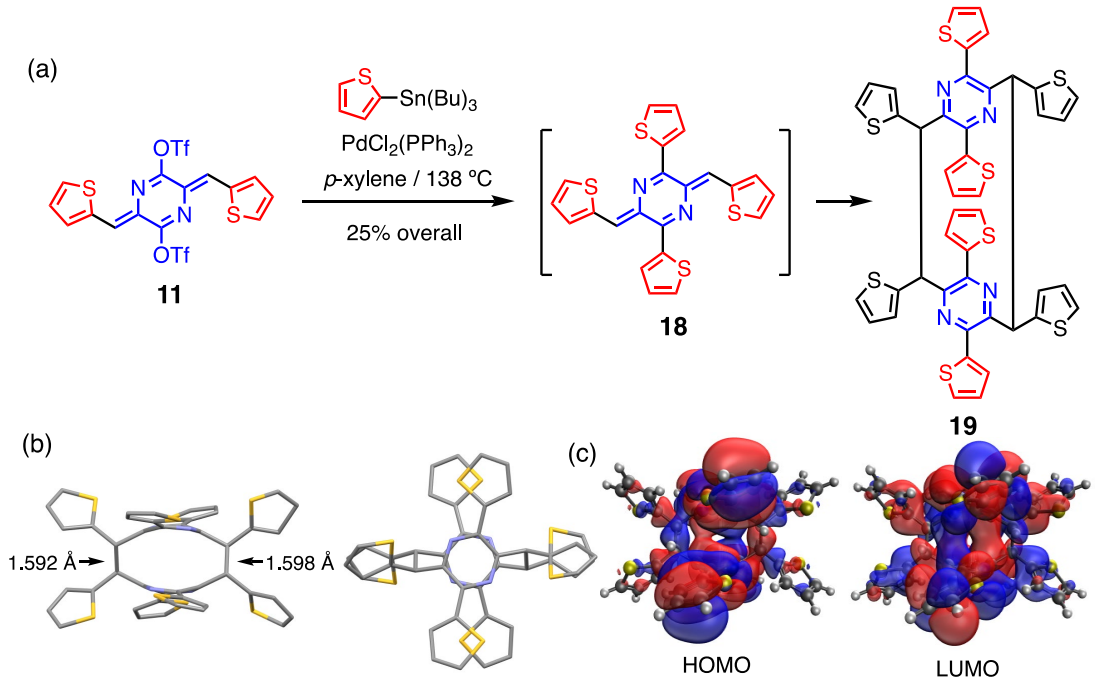

Scheme 5. (a) The synthesis of a highly substituted [2.2]paracyclophane **19** from AQM triflate **11**. (b) Single crystal X-ray structure of **19**. (c) Frontier molecular orbital plots showing the through-space conjugation within **19**. Adapted with permission from ref 36. Copyright 2020 The Royal Society of Chemistry.

4.3 Topochemical polymerization (TCP) of AQM ditriflates to form ultra-high molecular weight polymers

The intricacy of reactivity of AQMs is further demonstrated in AQM ditriflates that bear phenyl ring systems as the aromatic end groups instead of thiophenes. AQM triflate **12** is readily obtained in high yield (Scheme 3), but unlike its thiophene-derived homologue **11**, **12** is capable of

spontaneous polymerization under light or heat in the crystalline state.[3] The polymerization suggests a somewhat greater biradical reactivity of the phenyl end-capped AQM triflates, which has prompted us to investigate their topochemical reactivity in the crystalline states. When single crystals of **20** were subjected to sunlight or visible light irradiation (Figure 5a), topochemical polymerization occurred readily, as indicated by a color change in the crystals from yellow to white and the loss of solubility. Although it has been difficult to obtain suitable polymer single crystals for X-ray diffraction structural determination, satisfactory atomic structural details of the polymer were obtained through microelectron diffraction (μ-ED) transmission electron microscopic (TEM) studies of sub-micron sized crystalline samples of **P15**. Analysis of the single crystal structure of **20** and the corresponding polymer **P15** revealed "reactive" packing features that are prerequisites for topochemical polymerization.[38] In the monomer crystals, the central AQM unit is highly coplanar with its phenyl end groups, which results in slipped stacking of **20** in extended columns in a head-to-tail fashion, with close π-π interplanar distance around 3.4 Å. The distances between the active methylene carbons on neighboring AQM monomers in the solid state (d_{CC}s) are around 3.6 Å. Such molecular arrangement ideally sets the stage for the propagation of new C-C bond formation through intermolecular 1,6-addition with minimal relocation of atoms required upon polymerization, and thus macroscopic crystal integrity is largely preserved and ultra-high molecular weight (Mn $\geq 10^6$ g/mol) polymers can be produced.[39-41] The triflate groups on the central pyrazine rings remain intact during the polymerization, and it was hypothesized that these could be used to install chemical functionality after the initial polymerization.

To evaluate the fidelity of the polymerization, we made use of solubilizing 3,5-dihexyloxyphenyl end groups on the AQM ditriflate monomers. This monomer crystalizes into the preferred reactive packing mode and polymerizes readily, showing that these diphenyl AQM

ditriflates tolerate structural modification and still successfully undergo topochemical polymerization, a feature that is not observed in analogous tetrasubstituted *p*-QM systems reported by Itoh and coworkers.[40, 42] The resulting polymer **P16** displayed high solubility in common organic solvents, allowing for solution-based polymer characterization, post-synthetic modification, and thin film processing, which have been a rarity for topochemical polymers. Size exclusion chromatographic studies show that **P16** could be obtained at ultra-high molecular weights (Figure 5b). Capacitors based on dropcast films of **P16** displayed a high discharged energy density of 8.54 J cm^{-3}, a high breakdown strength of 568 MV m^{-1} and high charge–discharge efficiencies (> 97% at 200 MV m^{-1}), which significantly exceeds the behavior of the benchmark biaxially-oriented polypropylene (BOPP) and the structurally similar poly(para-xylylene) polymer, Parylene C (Figure 5c). The high energy density can be attributed to the high effective dielectric constant of the polymer (K = 8.14) due to the presence of the rotatable and highly polar triflate groups within the polymer repeat structure. Further efforts on post-polymerization functionalization of **P16** demonstrate that, despite the steric crowding caused by the bulky 3,5-disubstituted phenyl groups, the triflates could be replaced in acceptable yields via nucleophilic substitution with primary and secondary amines,[3] and presumably other simple nucleophiles.

The topochemical reactivity of AQM derivatives provides access to polymers with diverse structures and functions. The solution processibility of the polymer product, imbued by the high fidelity of the packing motif and reactivity of AQMs in the solid state, enables TCP reactions as a practical tool for polymer chemists, opening up applications that were previously inaccessible. Additionally, the unique reactivity of phenyl-capped AQM ditriflates implies that the aryl end groups extending from the AQM ring can be used to affect the extent of the AQM ring's quinoidal reactivity.

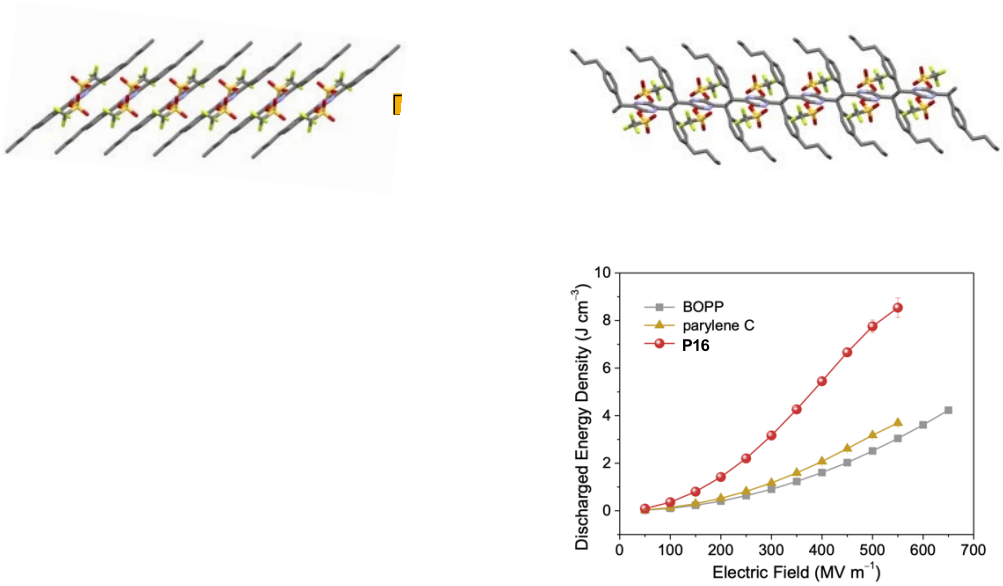

Figure 5. (a) TCP of AQM monomer **20**, together with the single crystal structures of the monomer **20** (by X-ray diffraction) and the polymer **P15** (by microED). (b) A soluble polymer **P16** obtained from an analogous TCP. (c) Dielectric energy storage properties of capacitors based on solution-processed films of **P16**. Adapted with permission from ref 3. Copyright 2021 the authors. Published by Springer Nature under a Creative Commons Attribution 4.0 International License (http://creativecommons.org/licenses/by/4.0/)

4.4 Pentacyclic electron donors by intramolecular cyclization of iAQMs

The quinoidal-type reactivity of the central AQM ring systems is significantly altered when the original thiophene end groups are replaced with phenyl derivatives in AQM ditriflates. In addition to the aforementioned topochemical reactivity, we have discovered that the increased reactivity

can also be harnessed to construct a novel aromatic pentacycle featuring the pyrazino[2,3-*b*:5,6-*b'*]diindolizine (PDIz) ring system through a succinct reaction sequence.[43]

The pentacyclic PDIz core was built atop the serendipitous reactivity of the ionic AQM intermediate, **21**, which was obtained from the nucleophilic displacement reaction between **12** and pyridine (Figure 6a). In contrast to its thiophene analog, **13**, the pyridinium displacement product underwent a spontaneous intramolecular cyclization to produce the substituted pyrazino[2,3-*b*]indolizine **22** in high yield. It was hypothesized that a second ring closure could be promoted to form the symmetrical PDIz framework. To accomplish this, a cascade reaction was devised, involving a base-promoted intramolecular cyclization and subsequent dehydrogenative aromatization to produce the highly planar **PDIz:H** (**23**), the structure of which was confirmed by single crystal X-ray diffraction (Figure 6b). Electrochemical studies indicated a very low HOMO energy level of -4.7 eV and a narrow electrochemical band gap of 1.90 eV, in accordance with the observed narrow optical band gap (Figure 6c). Due to its rich redox properties, **PDIz:H** is electrochromic and readily forms ground state charge-transfer complexes with electron acceptors. Despite the fact that it is highly electron-rich and possesses extended conjugation, **23** boasts a much greater stability towards oxygen than the isoelectronic pentacene, showing no noticeable degradation in the solid state under ambient conditions and only exceedingly slow degradation in solution.

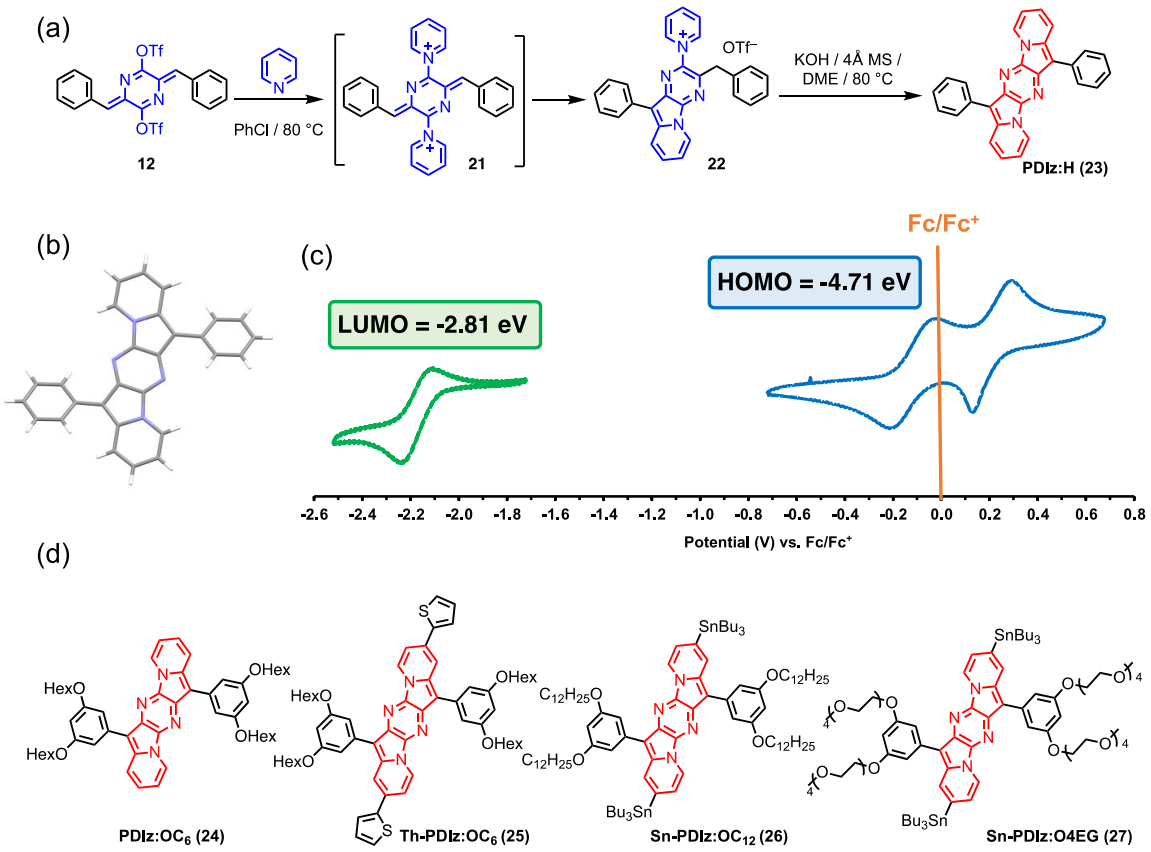

Figure 6. (a) Synthesis and (b) single crystal X-ray structure of a pentacyclic electron donor **PDIz:H** (**23**). (c) Electrochemistry revealing the electrochemical band gap and the low-lying HOMO energy level of **PDIz:H** (**23**). (d) A range of functionalized **PDIz** derivatives obtained following the synthetic protocol. Adapted with permission from ref 43. Copyright 2023 American Chemical Society.

A range of PDIz derivatives can be obtained following the same reaction sequence (Figure 6d), allowing for the installation of solubilization side chains as well as reactive stannate groups. The high ambient stability of PDIz compounds renders them a rare super electron-rich building block for the synthesis of narrow band gap conjugated polymers when combined with suitably

strong electron acceptors. Polymers **P17**–**P21** with widely varying electronic structures and side-chain polarities were synthesized via Stille coupling (Figure 7a), including those with absorbances in the biologically relevant NIR-I and -II regions. Among them, polymers **P17** and **P18** containing a benzobisthiadiazole (BBT) electron acceptor show ultra-narrow band gaps reaching ~0.7 eV. These polymers exhibited superior photothermal conversion efficiencies that are effective for laser ablation of cancer cells using a NIR-II laser, demonstrating their promise as deep-tissue photothermal therapeutic reagents.[44] The AQM-derived PDIz system fills an important void in the small group of narrow band gap organic redox-active strong electron-donor motifs. Its compatibility for incorporation into conjugated polymers opens the door to a wide range of band gap-tunable materials.

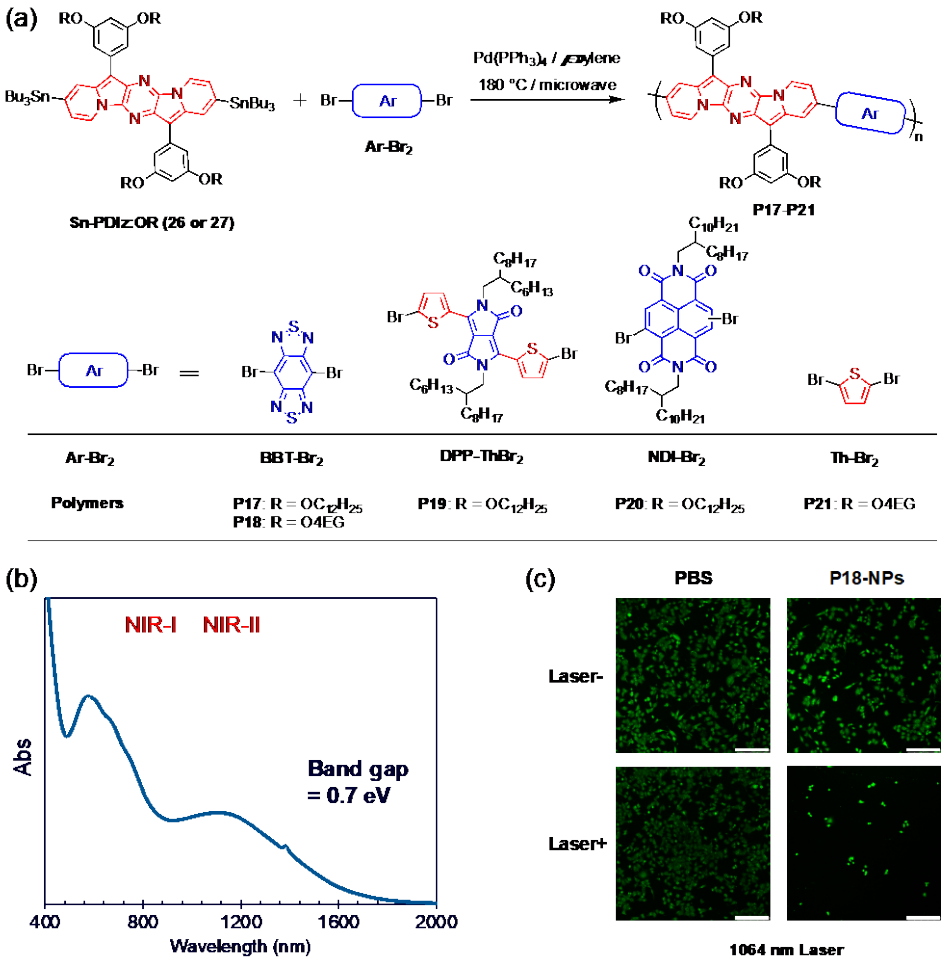

Figure 7. (a) Synthesis of narrow band gap donor-acceptor polymers using PDIz as the electron donor. (b) Absorption spectra of **P18** with an ultra-narrow band gap reaching 0.7 eV. (c) Confocal laser scanning microscopy images of living cells incubated with (left) and without (right) nanoparticles of **P18** upon NIR-II laser treatment (scalebar: 250 μm). Adapted with permission from ref 43. Copyright 2023 American Chemical Society.

5. Emerging properties: singlet fission materials

The dual closed-shell quinoidal/diradical aromatic nature of quinoidal compounds has garnered increasing attention in relation to singlet fission (SF), a spin-allowed process corresponding to the splitting of one singlet exciton into two triplet excitons via an internal conversion process.[45] Because of the multi-exciton generation upon single-photon photoexcitation and reduced thermalization losses, singlet fission is conducive to overcome the Shockley-Queisser limit in single-junction photovoltaic devices.[46] However, only a limited number of material classes exhibit high intramolecular SF efficiency and triplet harvest yield.[47] In particular, developing conjugated polymers capable of intramolecular SF and efficient dissociation of the resulting triplet pairs is a significant challenge.

AQM oligomers have been computationally predicted to be good candidates for SF, as their singlet ($E(S_1)$) and triplet state energies ($E(T_1)$) satisfy the requirement for exothermic SF energetics [$E(S_1) > 2E(T_1)$].[30, 48] Wang and coworkers have demonstrated that the AQM oligomer bearing a bithiophene on each side is a remarkable ambiently stable SF molecular material, with a suitable triplet energy of ~1.1 eV, an efficient SF process of t_{SF} ~3 ps and a triplet yield of 165%.[48] AQM-based conjugated polymer **P22** has also been experimentally identified as a highly efficient intramolecular SF material (Figure 8a).[30] Detailed transient absorption spectroscopic studies

revealed that triplet pairs were formed at an ultrafast rate (picoseconds) from the optically populated singlet state. In solution, the geminate triplet pairs recombine at a comparable rate, resulting in a very low triplet harvest yield. In contrast, in strongly coupled polymer thin films, the multiexcitons generated from intramolecular SF were able to diffuse and separate into long-lived free triplets with a triplet yield of 108% (Figure 8b and c). The efficient SF and triplet dissociation in the solid state of **P22** adds another dimension to both the fundamental photophysics of quinoidal compounds and their future applications as optoelectronic materials.

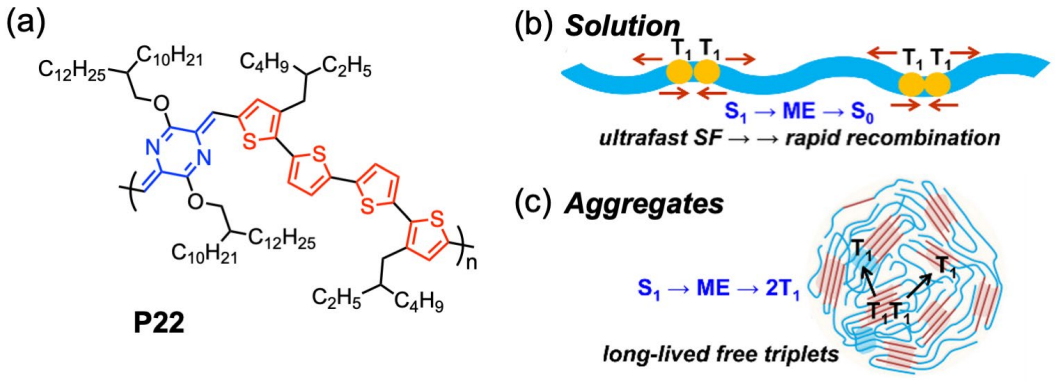

Figure 8. (a) Structure of the singlet fission polymer **P22**. Illustration of singlet fission processes in (b) solution and (c) aggregates. ME: multi-exciton generation. Adapted with permission from ref 30. Copyright 2020 American Chemical Society.

Summary and Outlook

Since the initial discovery of AQM as an electron-neutral quinoidal motif, it has become an enabling platform for understanding the unadulterated contribution of quinoidal character to the optoelectronic properties of conjugated systems, leading to the discovery of the reverse bandgap engineering rule in mixed quinoid-aromatic conjugated polymers. As research into the structure-morphology-performance relationships of these polymers has advanced, new conjugated polymers with desirable band gaps and exceptional charge transport properties have been discovered using

rational Q-D-A design principles. Such advances have inspired follow-up efforts that couple AQM units with specifically designed electroactive units and side chains to produce functional polymers with tunable optical, electronic and mechanical properties for uses in flexible electronics,[49] OFETs,[32, 50] organic photovoltaics[32, 51] and NIR bioimaging.[52-53]

One of the most remarkable aspects of AQMs beyond their inherent quinoidal character is their versatile but controllable reactivity. Unlike the prototypical *p*-QM, which is excessively reactive and thus cannot form stable conjugated systems, the reactivity of AQMs can be readily tuned to allow for straightforward transformation of the electron-neutral quinoid into either highly electron-deficient acceptors or extremely electron-rich donors. Consequently, AQMs can generate myriad unique building blocks for constructing functional conjugated polymers with unconventional ionic, redox and optical characteristics. Furthermore, the dormant diradicaloid reactivity of AQMs can be activated through different substitution patterns, as manifested by the formation of paracyclophanes and single-crystal-to-single-crystal topochemical polymerization.

The reactivity of the AQM motif that has been established thus far has only scratched the surface. There is still much to be learned about how to tune the balance between stable quinoid and latent or reactive biradicals, both experimentally and theoretically. The ability to precisely manipulate this balance, as hinted by the observed reactivity difference associated with different aromatic end groups, can serve as a springboard for the development of new open-shell aromatics and singlet fission materials with desirable optoelectronic properties and singlet-triplet gaps. The AQM example highlighted here is anticipated to inspire the discovery of new and potent quinoidal building blocks, paving the way for the development of materials with emerging properties.

AUTHOR INFORMATION

Corresponding Author

*Email: yliu@lbl.gov

Author Contributions

‡These authors contributed equally

Biographies

Xuncheng Liu was born in 1989 in Guizhou, China. He received his B.S. (2011), M.S. (2014) and Ph.D. (2017) degrees from South China University of Technology under the supervision of Professor Junwu Chen. He joined Yi Liu's Group at Lawrence Berkeley National Laboratory as a joint Ph.D. student during 2016 and 2017. He is now working at Guizhou University as a Distinguished Professor. His research interest focuses on the design and synthesis of organic semiconducting materials for field-effect transistors, solar cells and other electronic devices.

Christopher L. Anderson was born in 1992 in Sonoma, California. He received his B.S. from UC Santa Cruz in 2014 and his Ph.D. from UC Berkeley in 2020. Working in Yi Liu's group at Lawrence Berkeley National Laboratory, he studied the chemistry and applications of conjugated small band-gap organic materials and now works to advance the fields of carbon dioxide capture and sequestration.

Yi Liu is a Senior Staff Scientist at the Molecular Foundry, Lawrence Berkeley National Laboratory. He obtained his Ph.D. degree in Chemistry in 2004 from the University of California, Los Angeles, under the direction of Prof. Sir J. Fraser Stoddart. After his postdoctoral research with Prof. Barry Sharpless at the Scripps Research Institute, he joined the Molecular Foundry in 2006 as a Staff Scientist and has been directing the Organic and Macromolecular Synthesis Facility since 2016. His research interest involves organic electronics, porous frameworks, and organic-inorganic hybrids.

Acknowledgments

Y.L. thanks all the past and present group members who worked on AQMs: Bo He, Matthew Kolaczkowski, Jiatao Liang, Srikant Sagireddy, Chongqing Yang, Henry He Li, Ziman Chen, Miao Qi, and all the collaborators who contributed to the related studies. Y.L. acknowledges the support from the Molecular Foundry, a national user facility supported by the Office of Science, Office of Basic Energy Sciences, of the U.S. Department of Energy under Contract No. DE-AC02-05CH11231; and the support from the U.S. Department of Energy, Office of Science, Office of Basic Energy Sciences, Materials Sciences and Engineering Division, under Contract No. DE-AC02-05CH11231 within the Inorganic/Organic Nanocomposites Program (KC3104).

References:

1. Liu, X.; He, B.; Anderson, C. L.; Kang, J.; Chen, T.; Chen, J.; Feng, S.; Zhang, L.; Kolaczkowski, M. A.; Teat, S. J.; Brady, M. A.; Zhu, C.; Wang, L.-W.; Chen, J.; Liu, Y., para-Azaquinodimethane: A Compact Quinodimethane Variant as an Ambient Stable Building Block for High-Performance Low Band Gap Polymers. *J. Am. Chem. Soc.* **2017,** *139*, 8355-8363.
2. Anderson, C. L.; Dai, N.; Teat, S. J.; He, B.; Wang, S.; Liu, Y., Electronic Tuning of Mixed Quinoidal-Aromatic Conjugated Polyelectrolytes: Direct Ionic Substitution on Polymer Main-Chains. *Angew. Chem. Int. Ed.* **2019,** *58*, 17978-17985.
3. Anderson, C. L.; Li, H.; Jones, C. G.; Teat, S. J.; Settineri, N. S.; Dailing, E. A.; Liang, J.; Mao, H.; Yang, C.; Klivansky, L. M.; Li, X.; Reimer, J. A.; Nelson, H. M.; Liu, Y., Solution-processable and functionalizable ultra-high molecular weight polymers via topochemical synthesis. *Nat. Commun.* **2021,** *12*, 6818.
4. Liang, H.; Liu, C.; Zhang, Z.; Liu, X.; Zhou, Q.; Zheng, G.; Gong, X.; Xie, L.; Yang, C.; Zhang, L.; He, B.; Chen, J.; Liu, Y., Unravelling the Role of Electron Acceptors for the Universal Enhancement of Charge Transport in Quinoid-Donor-Acceptor Polymers for High-Performance Transistors. *Adv. Funct. Mater.* **2022,** *32*, 2201903.
5. Sun, Z.; Zeng, Z.; Wu, J., Zethrenes, Extended p-Quinodimethanes, and Periacenes with a Singlet Biradical Ground State. *Acc. Chem. Res.* **2014,** *47*, 2582-2591.
6. Casado, J., Para-Quinodimethanes: A Unified Review of the Quinoidal-Versus-Aromatic Competition and its Implications. *Top. Curr. Chem.* **2017,** *375*, 73.
7. Frederickson, C. K.; Rose, B. D.; Haley, M. M., Explorations of the Indenofluorenes and Expanded Quinoidal Analogues. *Acc. Chem. Res.* **2017,** *50*, 977-987.
8. Konishi, A.; Kubo, T., Benzenoid Quinodimethanes. *Top. Curr. Chem.* **2017,** *375*, 83.
9. Zeng, W.; Wu, J., Open-Shell Graphene Fragments. *Chem* **2021,** *7*, 358-386.
10. Burrezo, P. M.; Zafra, J. L.; Lopez Navarrete, J. T.; Casado, J., Quinoidal/Aromatic Transformations in π-Conjugated Oligomers: Vibrational Raman studies on the Limits of Rupture for π-Bonds. *Angew. Chem. Int. Ed.* **2017,** *56*, 2250-2259.
11. Hayashi, Y.; Kawauchi, S., Development of a quantum chemical descriptor expressing aromatic/quinoidal character for designing narrow-bandgap π-conjugated polymers. *Polym. Chem.* **2019,** *10*, 5584-5593.

12. Ji, X.; Fang, L., Quinoidal conjugated polymers with open-shell character. *Polym. Chem.* **2021,** *12*, 1347-1361.
13. Sun, Y.; Guo, Y.; Liu, Y., Design and synthesis of high performance π-conjugated materials through antiaromaticity and quinoid strategy for organic field-effect transistors. *Mater. Sci. Eng. R Rep.* **2019,** *136*, 13-26.
14. Huang, J.; Yu, G., Recent progress in quinoidal semiconducting polymers: structural evolution and insight. *Mater. Chem. Front.* **2021,** *5*, 76-96.
15. Mikie, T.; Osaka, I., Small-bandgap quinoid-based π-conjugated polymers. *J. Mater. Chem. C* **2020,** *8*, 14262-14288.
16. Kim, Y.; Hwang, H.; Kim, N.-K.; Hwang, K.; Park, J.-J.; Shin, G.-I.; Kim, D.-Y., π-Conjugated Polymers Incorporating a Novel Planar Quinoid Building Block with Extended Delocalization and High Charge Carrier Mobility. *Adv. Mater.* **2018,** *30*, 1706557.
17. Yang, M.; Du, T.; Zhao, X.; Huang, X.; Pan, L.; Pang, S.; Tang, H.; Peng, Z.; Ye, L.; Deng, Y.; Mingliang, S.; Duan, C.; Fei, H.; Yong, C., Low-bandgap conjugated polymers based on benzodipyrrolidone with reliable unipolar electron mobility exceeding 1 cm2 V− 1 s− 1. *Sci. China: Chem.* **2021,** *64*, 1219-1227.
18. Lahann, J.; Langer, R., Novel Poly(p-xylylenes): Thin Films with Tailored Chemical and Optical Properties. *Macromolecules* **2002,** *35*, 4380-4386.
19. Casado, J.; Ponce Ortiz, R.; López Navarrete, J. T., Quinoidal oligothiophenes: new properties behind an unconventional electronic structure. *Chem. Soc. Rev.* **2012,** *41*, 5672-5686.
20. Shi, X.; Chi, C., Heterocyclic Quinodimethanes. *Top. Curr. Chem.* **2017,** *375*, 68.
21. Zeng, Z.; Ishida, M.; Zafra, J. L.; Zhu, X.; Sung, Y. M.; Bao, N.; Webster, R. D.; Lee, B. S.; Li, R.-W.; Zeng, W., Pushing extended p-quinodimethanes to the limit: stable tetracyano-oligo (n-annulated perylene) quinodimethanes with tunable ground states. *J. Am. Chem. Soc.* **2013,** *135*, 6363-6371.
22. Liu, C.; Ni, Y.; Lu, X.; Li, G.; Wu, J., Global Aromaticity in Macrocyclic Polyradicaloids: Hückel's Rule or Baird's Rule? *Acc. Chem. Res.* **2019,** *52*, 2309-2321.
23. Kubo, T., Syntheses and Properties of Open-Shell π-Conjugated Molecules. *Bull. Chem. Soc. Jpn.* **2021,** *94*, 2235-2244.
24. Kawabata, K.; Saito, M.; Osaka, I.; Takimiya, K., Very Small Bandgap π-Conjugated Polymers with Extended Thienoquinoids. *J. Am. Chem. Soc.* **2016,** *138*, 7725-7732.
25. Deng, Y.; Sun, B.; He, Y.; Quinn, J.; Guo, C.; Li, Y., Thiophene‐S, S‐dioxidized Indophenine: A Quinoid‐Type Building Block with High Electron Affinity for Constructing n‐Type Polymer Semiconductors with Narrow Band Gaps. *Angew. Chem. Int. Ed.* **2016,** *55*, 3459-3462.
26. Rumer, J. W.; Rossbauer, S.; Planells, M.; Watkins, S. E.; Anthopoulos, T. D.; McCulloch, I., Reduced roughness for improved mobility in benzodipyrrolidone-based, n-type OFETS. *J. Mater. Chem. C* **2014,** *2*, 8822-8828.
27. Cui, W.; Yuen, J.; Wudl, F., Benzodipyrrolidones and Their Polymers. *Macromolecules* **2011,** *44*, 7869-7873.
28. Gallina, C.; Liberatori, A., Condensation of 1,4-diacetylpiperazine-2,5-dione with aldehydes. *Tetrahedron* **1974,** *30*, 667-673.
29. Wang, X.; Wang, K.; Wang, M., Synthesis of conjugated polymers via an exclusive direct-arylation coupling reaction: a facile and straightforward way to synthesize thiophene-flanked benzothiadiazole derivatives and their copolymers. *Polym. Chem.* **2015,** *6*, 1846-1855.
30. Wang, L.; Liu, X.; Shi, X.; Anderson, C. L.; Klivansky, L. M.; Liu, Y.; Wu, Y.; Chen, J.; Yao, J.; Fu, H., Singlet Fission in a para-Azaquinodimethane-Based Quinoidal Conjugated Polymer. *J. Am. Chem. Soc.* **2020,** *142*, 17892-17896.
31. Zhang, C.; Zhu, X., Thieno[3,4-b]thiophene-Based Novel Small-Molecule Optoelectronic Materials. *Acc. Chem. Res.* **2017,** *50*, 1342-1350.
32. Dyaga, B.; Mayarambakam, S.; Ibraikulov, O. A.; Zimmermann, N.; Fall, S.; Boyron, O.; Heiser, T.; Leclerc, N.; Berton, N.; Schmaltz, B., para-Azaquinodimethane based quinoidal polymers for opto-

electronic applications: impact of donor units on the opto-electronic properties. *Mater. Adv.* **2022,** *3*, 6853-6861.
33. Liu, X.; He, B.; Garzón-Ruiz, A.; Navarro, A.; Chen, T. L.; Kolaczkowski, M. A.; Feng, S.; Zhang, L.; Anderson, C. A.; Chen, J.; Liu, Y., Unraveling the Main Chain and Side Chain Effects on Thin Film Morphology and Charge Transport in Quinoidal Conjugated Polymers. *Adv. Funct. Mater.* **2018,** *28*, 1801874.
34. Liu, C.; Liu, X.; Zheng, G.; Gong, X.; Yang, C.; Liu, H.; Zhang, L.; Anderson, C. L.; He, B.; Xie, L.; Zheng, R.; Liang, H.; Zhou, Q.; Zhang, Z.; Chen, J.; Liu, Y., An unprecedented quinoid–donor–acceptor strategy to boost the carrier mobilities of semiconducting polymers for organic field-effect transistors. *J. Mater. Chem. A* **2021,** *9*, 23497-23505.
35. Chen, Z.; Khoo, R.; Garzón-Ruiz, A.; Yang, C.; Anderson, C. L.; Navarro, A.; Zhang, X.; Zhang, J.; Lv, Y.; Liu, Y., Quinoid-viologen conjugates: Redox properties and host-guest complex with cucurbiturils. *Mater. Today Chem.* **2022,** *24*, 100933.
36. Anderson, C. L.; Liang, J.; Teat, S. J.; Garzon-Ruiz, A.; Nenon, D. P.; Navarro, A.; Liu, Y., A highly substituted pyrazinophane generated from a quinoidal system via a cascade reaction. *Chem. Commun.* **2020,** *56*, 4472-4475.
37. Zafra, J. L.; Molina Ontoria, A.; Mayorga Burrezo, P.; Peña-Alvarez, M.; Samoc, M.; Szeremeta, J.; Ramírez, F. J.; Lovander, M. D.; Droske, C. J.; Pappenfus, T. M.; Echegoyen, L.; López Navarrete, J. T.; Martín, N.; Casado, J., Fingerprints of Through-Bond and Through-Space Exciton and Charge π-Electron Delocalization in Linearly Extended [2.2]Paracyclophanes. *J. Am. Chem. Soc.* **2017,** *139*, 3095-3105.
38. Cohen, M. D.; Schmidt, G. M. J., 383. Topochemistry. Part I. A survey. *J. Chem. Soc.* **1964**, 1996-2000.
39. Dou, L.; Zheng, Y.; Shen, X.; Wu, G.; Fields, K.; Hsu, W.-C.; Zhou, H.; Yang, Y.; Wudl, F., Single-Crystal Linear Polymers Through Visible Light–Triggered Topochemical Quantitative Polymerization. *Science* **2014,** *343*, 272.
40. Nomura, S.; Itoh, T.; Nakasho, H.; Uno, T.; Kubo, M.; Sada, K.; Inoue, K.; Miyata, M., Crystal Structures and Topochemical Polymerizations of 7,7,8,8-Tetrakis(alkoxycarbonyl)quinodimethanes. *J. Am. Chem. Soc.* **2004,** *126*, 2035-2041.
41. Hema, K.; Ravi, A.; Raju, C.; Pathan, J. R.; Rai, R.; Sureshan, K. M., Topochemical polymerizations for the solid-state synthesis of organic polymers. *Chem. Soc. Rev.* **2021,** *50*, 4062-4099.
42. Hema, K.; Ravi, A.; Raju, C.; Pathan, J. R.; Rai, R.; Sureshan, K. M., Topochemical polymerizations for the solid-state synthesis of organic polymers. *Chem. Soc. Rev.* **2021,** *50*, 4062-4099.
43. Anderson, C. L.; Zhang, T.; Qi, M.; Chen, Z.; Yang, C.; Teat, S. J.; Settineri, N. S.; Dailing, E. A.; Garzón-Ruiz, A.; Navarro, A.; Lv, Y.; Liu, Y., Exceptional Electron-Rich Heteroaromatic Pentacycle for Ultralow Band Gap Conjugated Polymers and Photothermal Therapy. *J. Am. Chem. Soc.* **2023,** *145*, 5474-5485.
44. Lyu, Y.; Li, J.; Pu, K., Second Near-Infrared Absorbing Agents for Photoacoustic Imaging and Photothermal Therapy. *Small Methods* **2019,** *3*, 1900553.
45. Smith, M. B.; Michl, J., Singlet Fission. *Chem. Rev.* **2010,** *110*, 6891-6936.
46. Rao, A.; Friend, R. H., Harnessing singlet exciton fission to break the Shockley–Queisser limit. *Nat. Rev. Mater.* **2017,** *2*, 17063.
47. Low, J. Z.; Sanders, S. N.; Campos, L. M., Correlating Structure and Function in Organic Electronics: From Single Molecule Transport to Singlet Fission. *Chem. Mater.* **2015,** *27*, 5453-5463.
48. Wang, L.; Shi, X.; Feng, S.; Liang, W.; Fu, H.; Yao, J., Molecular Design Strategy for Practical Singlet Fission Materials: The Charm of Donor/Acceptor Decorated Quinoidal Structure. *CCS Chemistry* **2022,** *4*, 2748-2756.
49. Zhang, S.; Ocheje, M. U.; Huang, L.; Galuska, L.; Cao, Z.; Luo, S.; Cheng, Y.-H.; Ehlenberg, D.; Goodman, R. B.; Zhou, D.; Liu, Y.; Chiu, Y.-C.; Azoulay, J. D.; Rondeau-Gagné, S.; Gu, X., The Critical Role of Electron-Donating Thiophene Groups on the Mechanical and Thermal Properties of Donor–Acceptor Semiconducting Polymers. *Adv. Electron. Mater.* **2019,** *5*, 1800899.

50. Xiao, Y.; Fu, H.; Li, Z.; Zheng, Y.; Deng, P.; Lei, Y.; Yu, Y., 6H-[1,2,5]Thiadiazolo[3,4-e]thieno[3,2-b]indole-flanked para-azaquinodimethane based aromatic-quinoidal polymer semiconductors with high molecular weights synthesized via direct arylation polycondensation. *Mat. Adv.* **2023**, *4,* 1927-1934.
51. Yang, Q.; Gong, X.; Qi, X.; Liu, X.; Liu, C.; Zhou, Q.; Sun, Q.; Shen, Y.; Wang, M., Hydrophobic polymer interlayer for highly efficient and stable perovskite solar cells. *Chem. Eng. J.* **2023,** *454*, 140430.
52. Su, Y.; Miao, Y.; Zhu, Y.; Zou, W.; Yu, B.; Shen, Y.; Cong, H., A design strategy for D–A conjugated polymers for NIR-II fluorescence imaging. *Polym. Chem.* **2021,** *12*, 4707-4713.
53. Miao, Y.; Gu, C.; Yu, B.; Zhu, Y.; Zou, W.; Shen, Y.; Cong, H., Conjugated-Polymer-Based Nanoparticles with Efficient NIR-II Fluorescent, Photoacoustic and Photothermal Performance. *ChemBioChem* **2019,** *20*, 2793-2799.